correlations within σ bonds involving empty e_g orbitals are reduced by the factor J_{intra}/U' to give the relative strengths indicated.

3. Polarization Superexchange

The polarization mechanism consists of an induced spin polarization of a doubly occupied core orbital by admixture of an unoccupied atomic valence orbital. Keffer and Oguchi[10] used nonorthogonal orbitals and obtained a sizeable effect since some delocalization and correlation superexchange were thereby included. If orthogonal orbitals are used throughout, the various polarization mechanisms[9,10] turn out to be inconsistent with the form of Eq. (2), but considerably smaller than the correlation and delocalization superexchange.[22]

3d Band Structure of Cr

M. Asdente
Laboratori CISE, Milano, Politecnico di Milano, Milan, Italy

AND

J. Friedel
Physique des Solides, Faculté des Sciences, Orsay (Seine et Oise), France
(Received April 26, 1961)

The electronic structure of the 3d band in Cr is calculated in the tight-binding approximation; the effect of the nearest-neighbor interaction and of the second-nearest-neighbor interaction on the energy surfaces in the Brillouin zone and on the density-of-states curve $g(E)$ is investigated.

By means of group theory, an analysis of the electron levels and of the eigenfunctions is performed in some particular points of the Brillouin zones; bonding and antibonding characters are found, together with different space distributions, for the eigenfunctions at the bottom and at the top of the band.

A comparison with other theoretical results suggests that the details of the chosen potential do not influence the general trend of the $g(E)$ curve very much; also satisfactory is a comparison with experimental results (particularly concerning electronic specific heat C_v, magnetic susceptibility χ, and thermoelectric power).

INTRODUCTION

THE central problems concerning transition metals are the determination of energy level distribution, the knowledge of the related wave functions, and the space density of charge. The properties observed along the three series of transition metals, particularly the electronic specific heat C_v and the magnetic susceptibility χ, suggest a high density of states at the Fermi level for most of them and the presence of some peaks in the density-of-states curve $g(E)$ as a function of energy. Theoretically, a self-consistent solution of the problem is prohibitively hard; a number of approximations must be made to make the problem manageable and one cannot always foresee exactly how much uncertainty each approximation introduces.

Nevertheless some results obtained so far by different methods[1-3] are satisfactory at least qualitatively and a preliminary calculation also, even with drastic approximations, permitted Slater and Koster[4] to expect a minimum at the middle of the density-of-states curve for the bcc, as the low values of C_v and χ for Cr, Mo, and W suggest.

In this paper a calculation on the structure of the 3d band in Cr is made using the tight-binding approximation. The present calculation was performed to see the effect of the nearest- and second-nearest-neighbor interactions on the energy surfaces in the Brillouin zone and on the $g(E)$ curve, to investigate further, by comparison to the results of others, the influence of potential choice, and other comparisons of interest to both previous calculations and experimental results. Also, an analysis is given of the information that can be deduced by group theory about the electron levels and the eigenfunctions.

CALCULATION OF E(k) CURVES

A series of Bloch functions $\Phi_n(\mathbf{r},\mathbf{k})$ is built up starting from the five $f_n(\mathbf{r})$ normalized functions corresponding to the fivefold-degenerate 3d level of a single atom:

$$f_1=\frac{1}{N_1}xyf(r), \quad f_2=\frac{1}{N_1}yzf(r), \quad f_3=\frac{1}{N_1}zxf(r),$$

$$f_4=\frac{1}{N_2}(x^2-y^2)f(r), \quad f_5=\frac{1}{N_3}(3z^2-r^2)f(r), \quad (1)$$

$$\Phi_n(\mathbf{r},\mathbf{k})=\sum_l \exp(i\mathbf{k}\cdot\mathbf{R}_l)f_n(\mathbf{r}-\mathbf{R}_l), \quad n=1, 2, 3, 4, 5, \quad (2)$$

[1] G. C. Fletcher and E. P. Wohlfarth, Phil. Mag. 42, 106 (1951).
[2] E. F. Belding, Phil. Mag. 4, 1145 (1959).
[3] J. H. Wood, Phys. Rev. 117, 714 (1960).
[4] J. C. Slater and G. F. Koster, Phys. Rev. 94, 1498 (1954).

where **k** is the wave vector and R_1 the distance between the origin of coordinates and the atom in a position characterized by index l. Some linear combinations $\psi_i(\mathbf{k},\mathbf{r})$ of Bloch functions, built up as

$$\psi_i(\mathbf{r},\mathbf{k}) = \sum_{n=1}^{5} A_{n,i}\Phi_n(\mathbf{r},\mathbf{k}), \quad n, i = 1, 2, 3, 4, 5 \quad (3)$$

are assumed as wave functions for the electrons in the crystal.

Mixing with the $4s$ states is neglected; it is most probably weak, as the density of states for the $4s$ band is low in the $3d$ band range of energy and therefore the weak s character introduced by this overlapping is believed not to modify appreciably the d-band structure.

Making use of the Ritz[5] variational method and the tight-binding approximation,[6] the secular equation is derived:

$$|H_{nm}(\mathbf{k}) - E(\mathbf{k})\delta_{nm}| = 0, \quad n, m = 1, 2, 3, 4, 5 \quad (4)$$

where

$$H_{nm} = E_0\delta_{nm} + C_{nm}\delta_{nm} + \sum_{l \neq 0}' \exp(i\mathbf{k}\cdot\mathbf{R}_1)$$

$$\times \int f_n(\mathbf{r}-\mathbf{R}_1)[V(\mathbf{r}) - V_0]f_m(\mathbf{r})d\tau,$$

E_0 is the fivefold-degenerate energy of the single atom, $C_{nm} = \int f_n(\mathbf{r})[V(\mathbf{r}) - V_0]f_m(\mathbf{r})d\tau$, $V(\mathbf{r})$ is the crystalline potential, and V_0 is the potential of the atom in the origin. The $f_n(\mathbf{r})$ functions have been determined by deducing the radial portion $f(r)$ from Slater's atomic functions.[7] $V(\mathbf{r})$ has been constructed with a set of Coulomb-like atomic potentials; around each lattice point $\mathbf{R}_1$ we have set

$$V(\mathbf{r}) = 4.6\left(\frac{1}{|\mathbf{r}-\mathbf{R}_1|} - \frac{1}{d/2}\right) \quad \text{for} \quad |\mathbf{r}-\mathbf{R}_1| \leqslant d/2,$$
$$V(\mathbf{r}) = 0 \quad \text{for} \quad |\mathbf{r}-\mathbf{R}_1| > d/2, \quad (5)$$

where d is the distance between nearest neighbors and the figure 4.6 is the effective nuclear charge obtained by the Slater's rules,[7] an outer electronic structure d^5s^1 being assumed for atomic Cr. In addition we have assumed

$$V(\mathbf{r}) - V_0 = 0 \quad \text{for} \quad |\mathbf{r}| \leqslant d/2,$$
$$V(\mathbf{r}) - V_0 = V(\mathbf{r}) \quad \text{for} \quad |\mathbf{r}| > d/2. \quad (6)$$

The above secular equation has been solved for $E(\mathbf{k})$ at a series of points in the Brillouin zone by an electronic ΓET Olivetti Bull computer using two separate approximations.

[5] C. A. Coulson, *Valence* (Clarendon Press, Oxford, England, 1953), 2nd ed., p. 61.
[6] N. F. Mott and H. Jones, *The Theory of the Properties of Metals* (University Press, Oxford, England, 1958), p. 65.
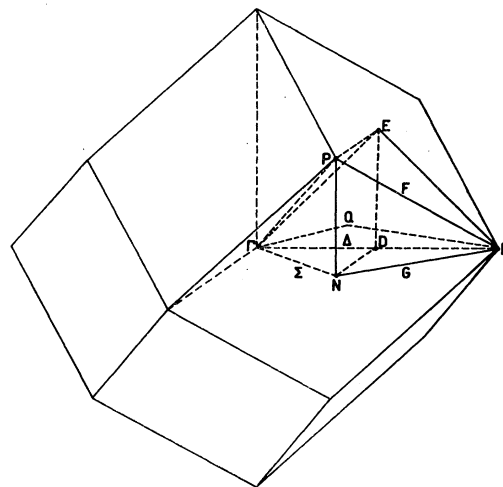[7] J. C. Slater, Phys. Rev. **36**, 57 (1930).

Fig. 1. Brillouin zone for bcc lattice.

In the first approximation only the nearest-neighbor interactions were considered, and in the second approximation the effect of the second-nearest neighbors was added to the first solution; in all cases the three-center integrals have been neglected. These two approximations will be referred to as AI and AII, respectively.

The values for $E(\mathbf{k})$ have been obtained along a series of lines ΓQ and QH shown in Fig. 1, where Q can vary on the square marked $NDPE$. In the cases where only the interactions between nearest neighbors are considered and the dependence of C_{nn} integrals upon the index n is neglected, the secular equation exhibits some properties of symmetry in pairs of points that are symmetrical with respect to the square $NDPE$ (Fig. 1). This symmetry makes one expect the values of $E(\mathbf{k})$ to be equal and opposite at these points. Some calculations have already been made with these approximations.[1,4] On the other hand, the different symmetries which $f_n(\mathbf{r})$ exhibits for $n=1$, 2, 3 and for $n=4,5$ suggest a certain dependence of C_{nn} upon n, depending of course on the potential $V(\mathbf{r})$ chosen. In the present calculation we have obtained $C_{11} = C_{22} = C_{33} \simeq 3C_{44} = 3C_{55}$, and thus it seemed convenient to find solutions for the whole Brillouin zone, and in particular along the lines symmetrical with respect to the square $NDPE$.

Figures 2–5 show, respectively, the trend of $E(\mathbf{k})$ along the lines of peculiar symmetry ΓH, $\Gamma N - NH$, $\Gamma P - PH$ for both the AI and AII approximations while Fig. 5 shows it along a general line $\Gamma Q - QM$.

The difference in the trend of the curves AI and AII, not large in general, will be examined later. It can be seen in AI that the integrals C_{nn} have affected the symmetry by a larger extent than the interaction between the second-nearest neighbors, as it is shown by a comparison of AI with AII. It is interesting to compare the curves AI in Figs. 2–4 with those by Slater and Koster [Fig. 2 (a, b, c) of reference 4]. The integrals C_{nn} not
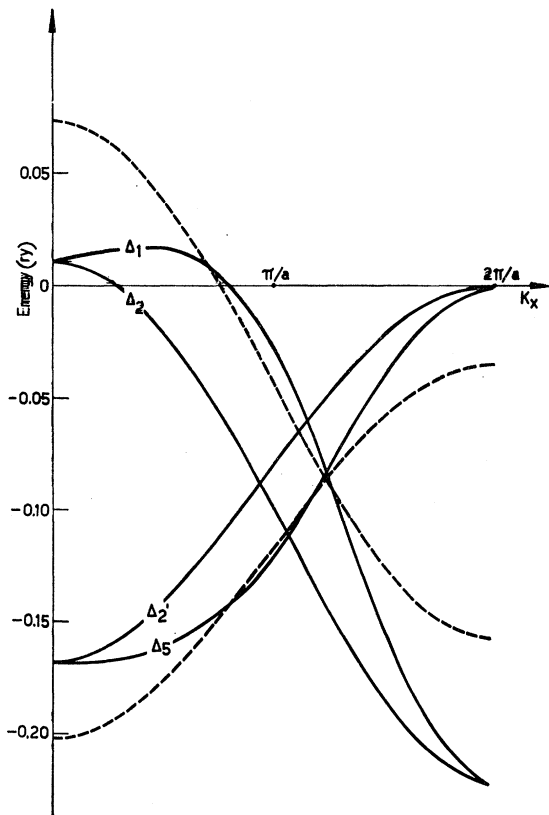
FIG. 2. Energy bands $E(\mathbf{k})$ along ΓH line. The dashed and the solid curves represent, respectively, the results obtained in the AI and in the AII approximation.

only have caused a destruction of the symmetry but have also given rise to lower values of $E(\mathbf{k})$ in general (the origin of the scale of energies is the same in both calculations) and have removed some degeneracy (for example, the fivefold degeneracy in P is separated into a twofold and threefold degeneracy).

GROUP-THEORETICAL ANALYSIS OF THE ELECTRON ENERGY LEVELS AND CRYSTAL WAVE FUNCTIONS

There exist well-established methods for obtaining some information about the properties of electron energy levels and crystal wave functions from group theory.[8] For each $\mathbf{k}$ value, the energy levels can be related to the irreducible representations (IR's) of the $G(\mathbf{k})$ group of the wave vector; the wave functions in the crystal are the bases of such IR. For a general $\mathbf{k}$ vector the only operation that transforms $\mathbf{k}$ in itself is the identity, which means that each crystal eigenstate is nondegenerate for that $\mathbf{k}$ (omitting the spin degeneracy and the possibility of an accidental one); if $\mathbf{k}$ has a particular symmetry, $G(\mathbf{k})$ can have a greater

order than one, and IR's with a greater order than one can exist.

To each m-fold degenerate IR can correspond one or more m-fold degenerate levels due to the contact of m bands. If the point in the Brillouin zone under consideration is moved from higher symmetry to lower symmetry, a degeneracy can be partially destroyed; such behavior can be investigated by the compatibility conditions between the IR's at such points.

Therefore, in the $\mathbf{k}$'s that have some symmetry properties it is possible to get some information on the d levels due to the type of functions shown in Eq. (3); any series of such functions can form the basis of what is in general a reducible representation (RR) of $G(\mathbf{k})$. The characters of this representation are easily obtained, and by means of the well-known tables of characters of the IR's of $G(\mathbf{k})$ the RR can be resolved into the IR components. In this way information about the degeneracy of levels, which would have been deduced from a proper series of Eq. (3) type functions, can be obtained. Moreover when the IR's which correspond to the levels considered are known, it is possible, by means of the projection operators, to take out from the functions chosen as bases of the RR those parts which transform themselves as a certain IR and to build up a set of basic functions for the same IR.

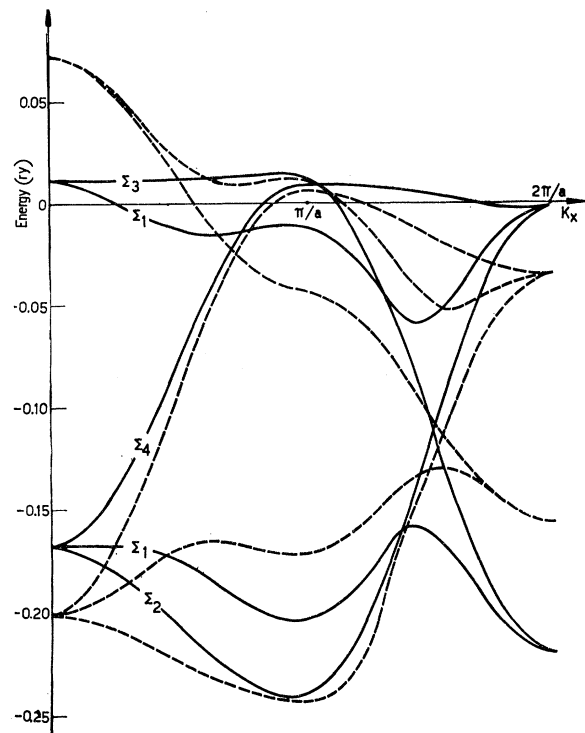Such an analysis has been carried out along the lines

FIG. 3. Energy bands along ΓN and NH lines. The point N corresponds to $k_x = \pi/a$. The dashed and the solid curves represent, respectively, the results obtained in the AI and in the AII approximation.

[8] See for instance: L. Bouckaert, R. Smoluchowski, and E. Wigner, Phys. Rev. 50, 58 (1936); G. F. Koster, Technical Report No. 8, Solid State and Molecular Theory Group, Massachusetts Institute Technology, 1956 (unpublished).

of the particular symmetries Δ, Λ, F, Σ, G (Fig. 1) in the Brillouin zone of the bcc lattice, assuming as bases of the RR the set of functions $\psi_n = \Phi_n$.

Figure 6 gives the IR's at the various points of the Brillouin zone, together with the relations derived according to the compatibility conditions at the points of different symmetry. (The symbols are the same as those used by Koster.[9] Conversion of Bouckaert, Smoluchowsky, and Wigner notation[8] can be made by interchanging the labels Σ_3 and Σ_4, and the labels N_3 and N_4.) The arrangement in this figure is merely formal and there is no connection with the actual order of the levels on the energy scale; in particular, the apparent crossings between the two Λ_3 IR's and two Σ_1 IR's are made simply to avoid the crossings between the corresponding energy levels. Even if the complete solution of the secular equation is not known, it is easy to verify that the order of the levels Γ_{12} and $\Gamma_{25'}$ is reversed at the points Γ and H; hence, for example, in order to avoid the crossing along the lines Λ and F of two levels Λ_3 of the same symmetry, it is necessary that in passing from Γ to H there is an interchange of the two Λ_3 IR's.

The behavior of the calculated Σ_1 levels in Fig. 3 and Λ_3 in Fig. 4 agrees with the above observations. In general, a proper arrangement of the degeneracies of the levels at the points and lines considered can be noticed in the curves AII in Figs. 2–4.
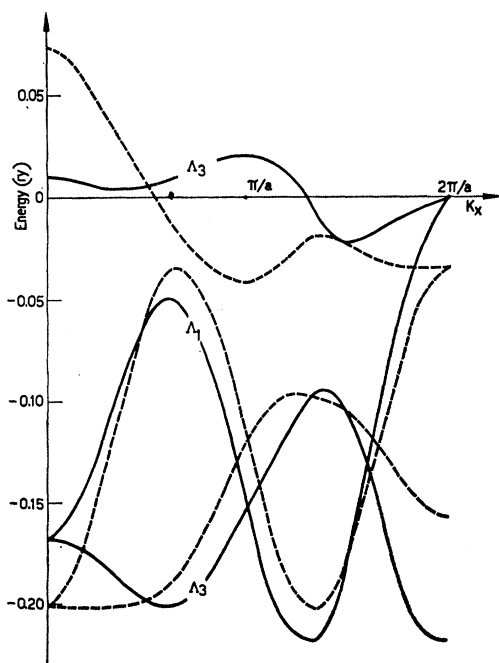

FIG. 5. Energy bands along ΓQ and QH lines. The point Q corresponds to $k_x = \pi/a$. The dashed and the solid curves represent, respectively, the results obtained in the AI and in the AII approximation.

FIG. 4. Energy bands along ΓP and PH lines. The point P corresponds to $k_x = \pi/a$. The dashed and the solid curves represent, respectively, the results obtained in the AI and in the AII approximation.

The analysis of the eigenfunctions by means of the projection operators gives the results shown in Table I.

Some difficulty was encountered for those $\mathbf{k}$'s in which the same IR appeared more than once, for in this case more than one functions of the same symmetry are obtained, a proper combination of which cannot be treated solely by group theory. This happens along the lines Σ and G for the two representations Σ_1, and along the lines Λ and F for the representations Λ_3; in these cases the orthogonal combinations whose eigenvalues are equal or very nearly equal to the $E(\mathbf{k})$ values calculated above were chosen.

The knowledge of the eigenfunctions of Table I, even if it does not give complete information for all the Brillouin zone, reveals some interesting properties of the wave functions. In particular it may be noted that the $3d$ band does not split into two parts corresponding to functions of different symmetry, as suggested by Mott and Stevens[10]; this is mainly due to the inversion in the order of Γ_{12} and $\Gamma_{25'}$ levels at the points Γ and H. It is also easy to see from the shape of the $E(\mathbf{k})$ solutions in such points that this is not due to the particular potential chosen but would be obtained from any reasonable potential.

Another feature of the wave functions that can be pointed out, taking into consideration the functions in Table I, is the different space distribution between the

[9] G. F. Koster, in Solid-State Physics, edited by F. Seitz and D. Turnbull (Academic Press, Inc., New York, 1957), Vol. 5, pp. 173–256.
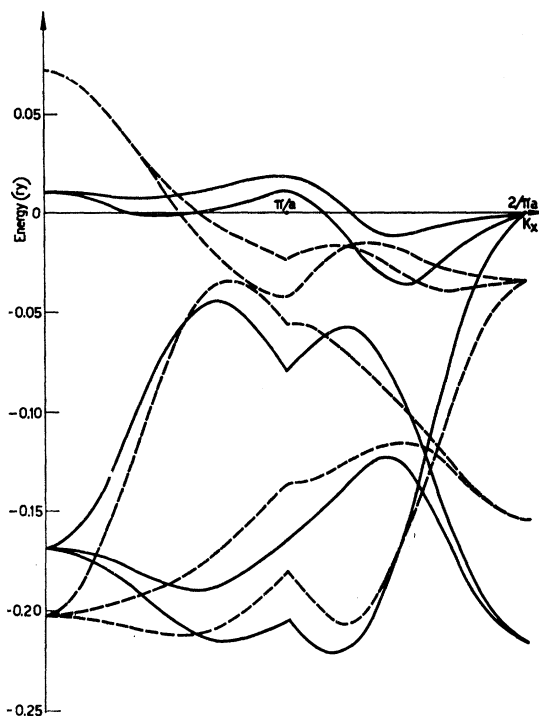
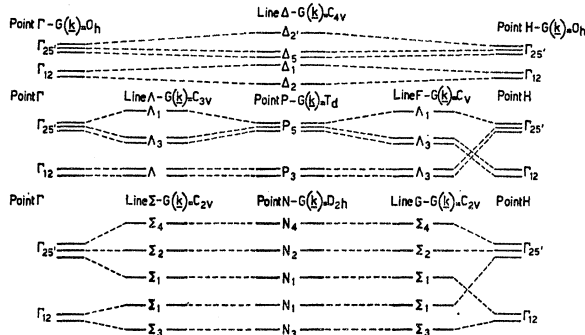[10] N. F. Mott and K. W. H. Stevens, Phil. Mag. 2, 1364 (1957).

FIG. 6. Irreducible representations relative to $3d$ band levels in the bcc lattice. The single, double, and triple lines show the order of the IR's and the degeneracy of the corresponding levels. [The symbols are the same as those used by Koster (reference 9)].

functions at the bottom and at the top of the band. Independently of their symmetry, the functions related to states at the bottom are widely expanded in the cell while those related to higher energies are characteristically contracted near the atoms. In the former the contributions to ψ_n due to the functions centered on the nearest-neighbor atoms are additive, while in the latter they cancel one another. It can be said that, starting from the bottom towards the top of the band, there is a gradual passage from bonding to antibonding states. These results are qualitatively similar to those found separately by Wood[3] and Stern[11] in iron with different methods[12]; they too find a transition from expanded functions to contracted ones when going from low to high energies. This feature can lead to a lower x-ray scattering factor than would be expected *a priori*, and

could eventually help to explain recent measurements on Cr and Fe.[13] In comparing the curves AI and AII in Figs. 2–4, an analogous relation can be noted between energy and the nature of the wave functions, in the sense that the energy levels regularly become lower or higher according to whether the corresponding functions have a bonding and antibonding character with respect to the next-nearest neighbor.

DENSITY-OF-STATES CURVE

The behavior of the density of states as a function of energy was obtained by graphic integration on the surfaces of constant energy in the Brillouin zone. The results from the two approximations AI and AII are shown in Figs. 7(a) and (b). The two curves show essentially similar behavior; the shape is analogous to that of the curve of Slater and Koster (Fig. 3 of reference 4) with the two peaks separated by a minimum. In

(a)

(b)

FIG. 7. Density-of-states curves $g(E)$; (a) AI approximation, (b) AII approximation. Open circles: $g(E_F)$ deduced from experimental values of C_v; solid points: $g(E_F)$ deduced from experimental values of χ.

TABLE I. Eigenfunctions chosen as bases of the IR's relative to $3d$ levels in Cr.

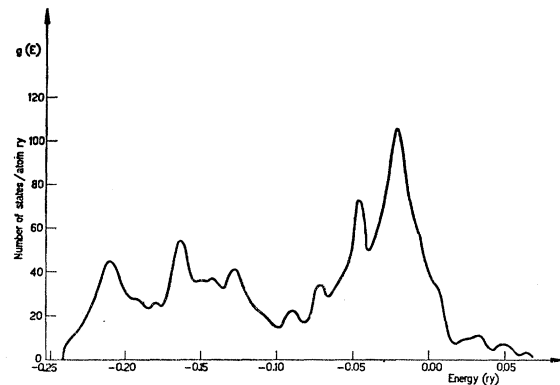| Points **k** in the Brillouin zone	IR	Basis functions
Point Γ	$\Gamma_{25'}$	$\psi_1; \psi_2; \psi_3$
	Γ_{12}	$\psi_4; \psi_5$
Line Δ	$\Delta_{2'}$	ψ_2
	Δ_5	$\psi_1; \psi_3$
	Δ_1	$3\psi_4 - \psi_5$
	Δ_2	$\psi_4 + \psi_5$
Lines Σ and G	Σ_4	$\psi_2 + \psi_3$
	Σ_2	$\psi_2 - \psi_3$
	Σ_1	$\psi_1 - (k_x a/2\pi)\psi_5, \quad 0 \le k_x \le \pi/a$
		$\psi_5 - [(2\pi - k_x a)/2\pi]\psi_1, \quad 3\pi/2a \le k_x \le 2\pi/a$
	Σ_1	$\psi_5 + (k_x a/2\pi)\psi_1, \quad 0 \le k_x \le \pi/a$
		$\psi_1 + [(2\pi - k_x a)/2\pi]\psi_5, \quad 3\pi/2a \le k_x \le 2\pi/a$
	Σ_3	ψ_4
Line Λ	Λ_1	$\psi_1 + \psi_2 + \psi_3$
	Λ_3	$\psi_1 - \psi_2; \psi_1 - \psi_2 + 2\psi_3$
	Λ_3	$\psi_4; \psi_5.$

[11] F. Stern, Phys. Rev. **116**, 1399 (1960).
[12] This result is in agreement also with the conclusions of a more general qualitative analysis made by G. Gousseland and G. Leman [J. phys. radium (to be published)] about the spatial electron distribution as deduced in the tight-binding approximation.
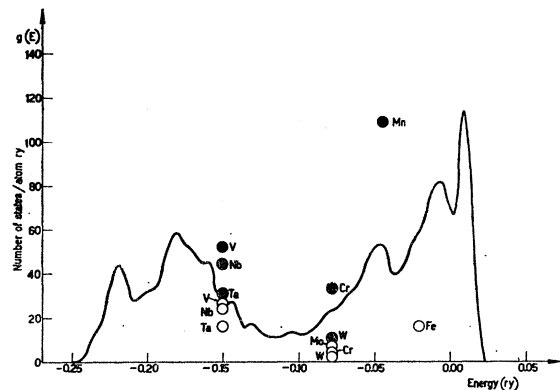
[13] W. Hume-Rothery, P. J. Brown, J. B. Forsyth, and W. H. Taylor, Phil. Mag. **3**, 1466 (1958); R. D. Deslattes, Phys. Rev. **110**, 1471 (1958); B. W. Batterman, Phys. Rev. Letters **2**, 47 (1959); B. W. Batterman, Phys. Rev. **115**, 81 (1959); B. W. Batterman, D. R. Chipman, and J. J. De Marco, Phys. Rev. **122**, 68 (1961).

our case, however, the fact that the integrals C_{nn} in the secular equation were taken into account has already resulted in a difference in the shape of the two peaks in curve AI as a direct consequence of the lack of symmetry in $E(\mathbf{k})$ curves mentioned earlier.

Moreover, the consideration of the interaction between the next-nearest neighbors leads to a narrower band, closer peaks, and a lower average energy, but no change in the general trend of the curve.

Furthermore, the shape of the curves does not seem to depend much on the hypothesis about the assumed $f_n(\mathbf{r})$ functions and potential; this is also suggested by a comparison with the results of a similar calculation on iron by Belding,[2] who also used the tight-binding method but started with the self-consistent atomic functions of Löwdin and Appel.[14] The $g(E)$ curve obtained by Belding shows a trend in agreement with the present results, particularly in regard to the width of the band which is of the same magnitude (about 4 ev) and in the existence of a higher peak at the top of the band. However, in passing from curves AI to AII, the long tail at low energies found by Belding does not appear. This indicates that this tail is an effect of the particular potential rather than of the interaction of the next-nearest neighbors as was suggested.[2]

Some information on the band structure can be obtained from experimental measurements. The density of states at the Fermi level can be deduced from the electronic specific heat and the electronic magnetic susceptibility, and the derivative of $g(E)$ can be obtained from the thermoelectric power. Figure 7(b) shows also the density of states deduced from the experimental values of[15] γ and[16] χ through the classical relations of the band theory[17]:

$$\gamma = C_v/T = \tfrac{2}{3}K^2\pi^2 g(E_F),$$

where $C_v =$ electronic specific heat for atom, $K =$ Boltzmann's constant, and $g(E_F) =$ density of states for atom at the Fermi level, and

$$\chi = 2\mu^2 g(E_F),$$

where $\chi =$ atomic susceptibility and $\mu =$ Bohr magneton.

In Fig. 7(b) the values deduced from χ are more or less proportional to those deduced from C_v, although they are somewhat larger. This difference is very probably due to the exchange interaction, as suggested by Mott,[18] and later demonstrated by Pines[19] in the

[14] P. Lowdin and K. Appel, Phys. Rev. **103**, 1746 (1956).
[15] R. Blaupain, Bull. Royale des Sciences de Liège, No. 4, 165 and 182 (1957).
[16] Values selected by C. J. Kriessman and H. B. Callen, Phys. Rev. **94**, 837 (1954).
[17] N. F. Mott and H. Jones, reference 6, p. 179 and p. 185.
[18] N. F. Mott and H. Jones, reference 6, p. 189.
[19] D. Pines, *Solid-State Physics*, edited by F. Seitz and D. Turnbull (Academic Press, Inc., New York, 1955), Vol. 1, pp. 368–450.
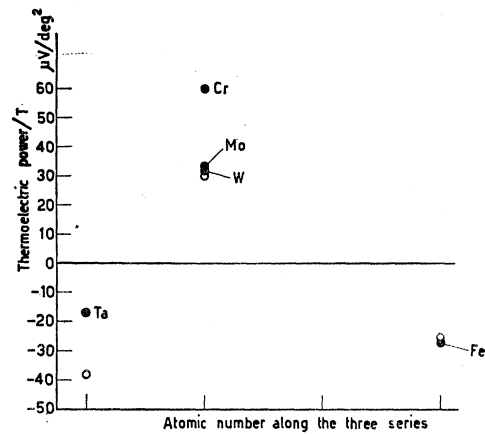
FIG. 8. Comparison between the experimental values of the thermoelectric power (solid points) and those deduced from curve of Fig. 7(b) (open circles).

hypothesis of the free electrons and by Stoner[20] for the transition metals.

A comparison with the experimental behavior along the whole range of the transition metals seems more reasonable than a comparison with one element only. For this reason, the values deduced for the other bcc metals of the three series are shown in Fig. 7(b) in addition to those deduced for Cr, with the assumption that the $g(E)$ curves are substantially similar for metals of equal structure. This assumption does not seem unreasonable in view of the small dependence of $g(E)$ on the type of potential mentioned earlier, and of the works of Bassani et al.[21] which emphasized the large influence of the lattice structure on the $E(\mathbf{k})$ curves.

In the absence of more exact information, some hypothesis had to be made about the position of E_F in the band for the various metals of the three series. The number of electrons occupying the band was assumed to vary linearly from 1 to 9.4 electrons/atom in passing from Sc, Y, La, respectively, to Ni, Pd, Pt. This gives therefore

3.4 electrons/atom for V, Nb, Ta;
4.6 electrons/atom for Cr, Mo, W;[22]
5.8 electrons/atom for Mn;
7 electrons/atom for Fe.

The agreement between the theoretical curve and the points deduced from experimental data is satisfactory. With the exception of Fe, which is ferromagnetic, a correct order of magnitude was found with respect to the values deduced from C_v for all other metals, and a correct behavior along the three series both with respect

[20] E. C. Stoner, Rept. Progr. Phys. **11**, 43 (1948), see also J. Friedel, Commissariat à l'Energie Atomique Report, CEA-766, 1958 (unpublished).
[21] F. Bassani, Phys. Chem. Solids **8**, 375 (1959); F. Bassani and V. Celli, Nuovo cimento **11**, 805 (1959).
[22] With this assumption the number of d electrons per atom in the case of Cr results a little smaller (4.6 instead of 5) than the one assumed to determine the effective nuclear charge.

to the values deduced from C_v and to those deduced from χ.

Recent experimental measurements[23] of electronic specific heat for V−Cr, Cr−Fe, and Fe−Co alloys have allowed to deduce the upper part of the density-of-states curve for the $3d$ band relative to bcc lattices (Fig. 15 of reference 23).

It is interesting to make a comparison between this curve and the one in Fig. 7b. Both curves show a peak comparable in height and width; in the experimental one, however, the peak is found at lower energy. For a discussion of the experimental results from which the curve in Fig. 15 of reference 23 has been deduced, we refer to the above-quoted paper.

Figure 8 shows a comparison between the experimental values of the thermoelectric power[24] and those deduced[25] from curve of Fig. 7(b). With the exception of the very high experimental value for Cr, a satisfactory agreement is obtained both with respect to sign as well as to the absolute value.

DISCUSSION OF APPROXIMATIONS USED

The above calculations employ several hypotheses and approximations which allow one to obtain more readily some information about the electron energy levels, eigenfunctions, and density of states.

Besides the usual hypotheses typical of the band theory and the tight-binding approximation, some other simplifications have been introduced. The more important ones are summarized below:

(1) The method of solution is not a self-consistent one; a spherically symmetrical potential in the neighborhood of each atom has been assumed *a priori*, and moreover the same potential has been assumed for all the states.

(2) Mixing with the $4s$ states has been neglected.

(3) The $3d$ eigenfunctions were not orthogonalized to the eigenfunctions of the core states.

It has already been remarked that it is difficult to

estimate how much these approximations influence the results. This influence can be estimated by comparison with other theoretical results, and with some experimental data, and by the analysis with group theory, the qualitative results of which, since they depend strictly upon the crystal structure and on the properties of symmetry, are less influenced by other peculiarities (the potential or the method of solution).

It seems apparent that C_{nn} integrals are not negligible because of their importance in determining the curves $E(\mathbf{k})$ and $g(E)$; but the magnitude of this effect can depend upon the potential chosen, for example, upon whether or not it is spherically symmetrical in the neighborhood of the atom. This may have some influence on the relative trend of the $E(\mathbf{k})$ curves corresponding to AI and AII approximations. In general in this calculation these curves show a similar trend; the greatest difference is, of course, for the electron states whose eigenfunctions are built up mainly with Φ_4 and Φ_5 functions. The eigenfunctions shown in Table I could be used to evaluate the effect on $E(\mathbf{k})$ of the interaction between next-nearest neighbors which would be obtained if a different potential were used.

Some of the conclusions in this paper seem to be more valid in general and less dependent upon the fundamental hypotheses and the approximations used in these calculations than those previously discussed.

The different spatial distribution of the eigenfunctions relative to the bottom and to the top of the band and their bonding and antibonding character, respectively, seem well established and supported by the results obtained by Wood and Stern, previously mentioned.

The potential chosen seems to have very little effect on the general trend of the $g(E)$ curve and can perhaps have a greater influence on the details of the shape and width of the curve.

[23] C. H. Cheng, C. T. Wei, and P. A. Beck, Phys. Rev. **120**, 426 (1960).
[24] G. Borelius, Handbuch der Metallphysik **1**, 181 (1934).
[25] N. F. Mott and H. Jones, reference 6, p. 310.